ORIGINAL ARTICLE

Recent Changes in Heavy Precipitation Events in Northern Central China and Associated Atmospheric Circulation

Tingting Han[1,2,3] · Xinyi Guo[1] · Botao Zhou[1,2,3] (ID) · Xin Hao[1,2,3]

Abstract

Northern Central China (NC China) is a seriously arid region. Precipitation variations are vital for environmental protection and socio-economical development. This study investigates the recent changes in summer heavy precipitation (HP) events over NC China and associated atmospheric circulation anomalies. Compared with the period of 1986–2002, the HP amount and frequency both significantly increase during 2003–2016, contributing to the shift to increase in total summer precipitation amount. After the early 2000s, the Northwest Pacific subtropical high becomes intensified and shifts westward and northward, leading to significant moisture convergence anomalies over NC China and divergence anomalies over Northwest Pacific. Therefore, the net moisture budget dramatically increases since the early 2000s. Further results show that the strengthened net moisture influx across the southern boundary contributes dominantly to the increased net moisture budget, especially at the lower level. Despite a relatively small magnitude, the intensified westerly current across western boundary makes a dominant contribution at middle and upper layers. Additionally, the strengthened westerly and easterly anomalies occupy northern and southern China, respectively, along with the eastward expansion of westerly jet stream region. Thus, the lower-level convergence and upper-level divergence both intensify, and further trigger enhanced ascending movement. These conditions jointly contribute to the inter-decadal change in HP events over NC China after the early 2000s.

Keywords Northern Central China · Heavy precipitation events · Decadal change · Moisture transport

1 Introduction

The northern region of Central China is located in the Loess Plateau. This region is one of the areas in China that has suffered from extremely serious soil erosion and has one of the most fragile ecological environments in the world. Climate change, especially precipitation variability, exerts great impacts on agricultural production, water resource management and social ecosystem development.

Northern Central China is situated at the edge of East Asian summer monsoon region. Summer precipitation variation in this region is influenced by regimes both in the tropics and extratropics, including the East Asian summer monsoon system (Ran et al. 2014), the sea surface temperature (referred to as SST) in critical areas (Jiang et al. 2009; Liu et al. 2013), the Arctic Oscillation (Wang et al. 2007) and arctic sea ice (Wang and Zhang 2010). Moreover, Wang and Fan (2005) found that the Antarctic Atmospheric Oscillation influences the atmospheric circulation and precipitation over northern Central China through the East Asia-Pacific tele-connection wave pattern. Xu et al. (2012) showed the leading influence of the North Atlantic Oscillation during June–August on the resulting September precipitation over Central China. In addition, Tan et al. (2014) indicated that the Pacific Decadal Oscillation affects precipitation in northern Central China by modulating the East Asia summer monsoon and the West Pacific Subtropical High.

✉ Botao Zhou
    zhoubt@cma.gov.cn

1 School of Atmospheric Sciences, Nanjing University for Information Science and Technology, Nanjing, China

2 Collaborative Innovation Center on Forecast and Evaluation of Meteorological Disasters/Key Laboratory of Meteorological Disaster, Ministry of Education, Nanjing University for Information Science and Technology, Nanjing, China

3 Nansen-Zhu International Research Centre, Institute of Atmospheric Physics, Chinese Academy of Sciences, Beijing, China

Korean Meteorological Society ⌖ Springer

The amount of extreme precipitation plays an important role in the total precipitation amount during summer over northern China (Wu and Fu 2013). Specially, strong rainfall amounts account for ~59% to total rainfall amounts in Northwest China, as documented by Chen and Dai (2009) wherein a strong rainfall event is defined based on the 85th percentile threshold of all rainy days. Despite supplementing water resources and agricultural irrigation, extreme precipitation events over northern Central China are generally liable to mountain torrents owing to unfavorable topo-geological conditions. Therefore, there are increasing concerns about the characteristics of extreme precipitation events and associated atmospheric circulation anomalies (Liu and Du 2006; Yuan et al. 2007; Xu et al. 2013). For example, Wan et al. (2014) stated prolonged return periods for rainstorms and heavy rainstorm events during 1957–2009. Sun et al. (2016) showed that the intensity of daily precipitation exhibited a significant increase during the last five decades. Previous studies have paid much attention to the interannual variation and long-term trend of extreme precipitation events over northern Central China, whereas few refer to the interdecadal variability, which is the central issue of this study.

Moisture transport significantly contributes to precipitation. During summer, moisture transport over China features three branches (Simmonds et al. 1999): the southerly current by the East Asia summer monsoon, which transports water vapor originating from the South China Sea and the tropical western Pacific, the southwesterly flow by the South Asia summer monsoon, which transports moisture deriving from the Bay of Bengal and the Arabian Sea, and the mid-latitude westerly carrying moisture from the Eurasian continent. The former two moisture transport branches bring abundant water vapor to the eastern, southern and northern regions of China, and the final branch to summer precipitation over northern China (Sun and Wang 2014, 2015a). Concurrently, Wei et al. (2010) showed that the moisture of northern Central China is mainly from the Bay of the Bengal, the South China Sea and the West Pacific. Previous studies have revealed the close relationship between the interdecadal variation in summer precipitation over East China and the interdecadal change in the moisture transport (Sun et al. 2011; Sun and Wang 2015b). Therefore, exploring the moisture transport anomalies associated with interdecadal variations of extreme precipitation events over northern Central China is essential.

The data and methods employed in this study are introduced in Section 2. Section 3 describes the interdecadal variation in extreme precipitation events and the associated moisture transport anomalies. The main conclusions are provided in Section 4.

2 Data and Methods

An advanced daily precipitation dataset (i.e., CN05.1) is used in this study from 1961 to 2016 (Wu and Gao 2013). This dataset is constructed by interpolating data from over 2400 observation stations at China, and has a relatively high resolution of $0.5° \times 0.5°$. This study focuses on summer heavy precipitation (HP) variation over northern Central China (32.5°–40°N, 100°–110°E; referred to as NC China), including the Shaanxi, Ningxia, southeastern Gansu and eastern Qinghai provinces. Summer refers to months of July, August and September.

The monthly global atmospheric reanalysis data are derived from the National Center for Environmental Prediction and the National Center for Atmospheric Research (NCEP/NCAR) with a resolution of $2.5° \times 2.5°$ for 1948–2016 (Kalnay et al. 1996), including sea level pressure, surface pressure, vertical motion, geopotential height, specific humidity, meridional and zonal winds at eight levels (1000, 925, 850, 700, 600, 500, 400, 300 hPa). The specific humidity and horizontal winds are used to calculate the moisture flux. The vertically integrated moisture flux is calculated between land surface and 300 hPa because water vapor above 300 hPa is tiny. The calculation of vertically integrated moisture flux (kg m^{-1} s^{-1}) is expressed as $\boldsymbol{Q} = \boldsymbol{Q}_\lambda \boldsymbol{i} + \boldsymbol{Q}_\varphi \boldsymbol{j}$. The zonal component is expressed as $\boldsymbol{Q}_\lambda = -\frac{1}{g}\int_{P_s}^{P_t}(qu)dp$, and the meridional component is expressed as $\boldsymbol{Q}_\varphi = -\frac{1}{g}\int_{P_s}^{P_t}(qv)dp$. In this equation, g is the gravity acceleration, with a value of 9.80665 (m s^{-2}), p_s is the bottom level pressure, p_t is the top level pressure, q is specific humidity, u and v are zonal and meridional winds, respectively. In addition, the vertical integration of water vapor across the four boundaries can be calculated as follows,

Southern boundary:

$$Q_s = \int_{\lambda_W}^{\lambda_E} \boldsymbol{Q}_{\varphi_S} a\cos\varphi_S d\lambda,$$

Northern boundary:

$$Q_N = -\int_{\lambda_W}^{\lambda_E} Q_{\varphi_N} a\cos\varphi_N d\lambda,$$

Western boundary:

$$Q_W = \int_{\varphi_S}^{\varphi_N} Q_{\lambda_W} a d\varphi,$$

Eastern boundary:

$$Q_E = -\int_{\varphi_S}^{\varphi_N} Q_{\lambda_E} a d\varphi.$$

The intensity index of the Northwest Pacific subtropical high comes from China's Meteorological Administration for 1961–2016. The common time period is set from 1961 to 2016 in this study.

Fig. 1 Time series of (**a**) proportion of heavy precipitation (abbreviated as HP) amount to summer total precipitation amount (%), (**b**) HP amount (mm), and (**c**) HP frequency (days) averaged within northern Central China (abbreviated as NC China; 32.5°–40°N, 100°–110°E) for the period 1961–2016 (bar) and 7-year moving mean (solid line). (**d**) Moving *T* test for the heavy precipitation amount at NC China. The red, blue, and green dotted lines denote the significance level at $\alpha = 0.10$, 0.05, and 0.01, respectively
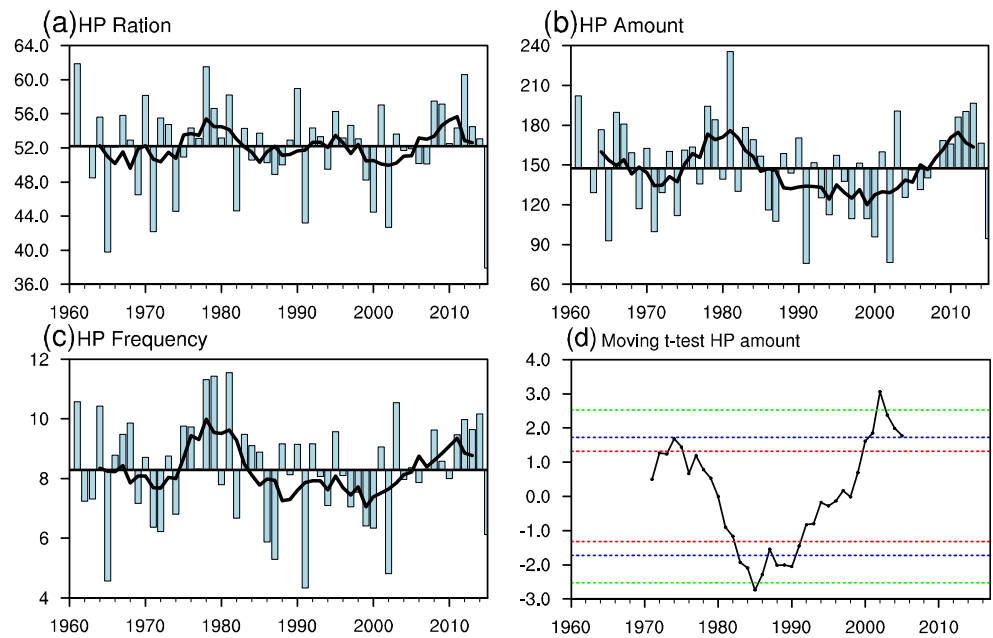
In this study, a HP event is defined as an event with daily precipitation rate exceeding the 90th percentile threshold of all rainy days (daily precipitation larger than 0.1 mm) during summer half year from 1961 to 2016.
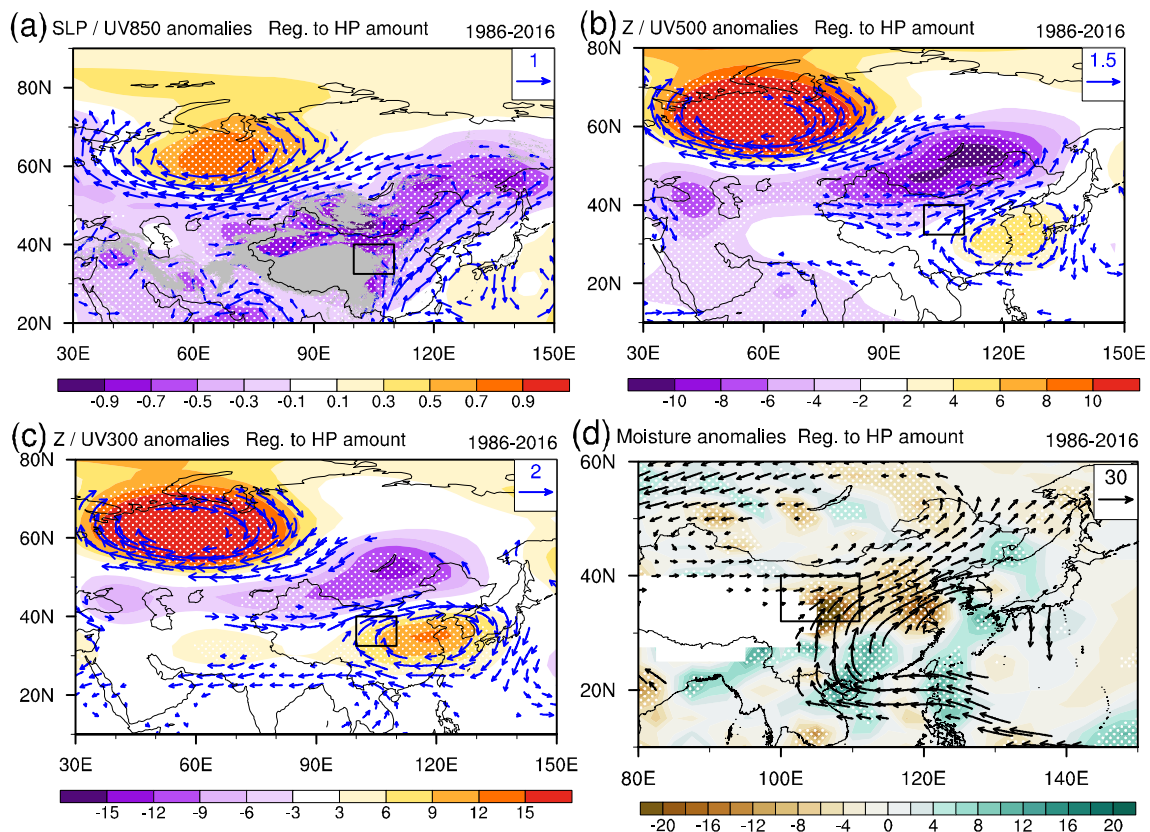
Fig. 2 Linear regression of (**a**) sea level pressure (SLP; shaded; mb) and horizontal wind at 850 hPa (vectors; m s^{-1}), (**b**) 500 hPa geopotential height (shaded; m) and horizontal wind (vectors; m s^{-1}), (**c**) 300 hPa geopotential height (shaded; m) and horizontal wind (vectors; m s^{-1}), and (**d**) vertically integrated moisture flux from surface to 300 hPa (kg m^{-1} s^{-1}) with regard to HP amount over NC China during summer from 1986 to 2016. Vectors that are significant at the 90% confidence level are plotted. Stippling areas indicate values that significantly exceed the 90% confidence level, estimated using Student's *t* test. The rectangle represents the NC China

Table 1 Years characterized by decreased HP amount during 1986–2002 and increased HP amount during 2003–2016

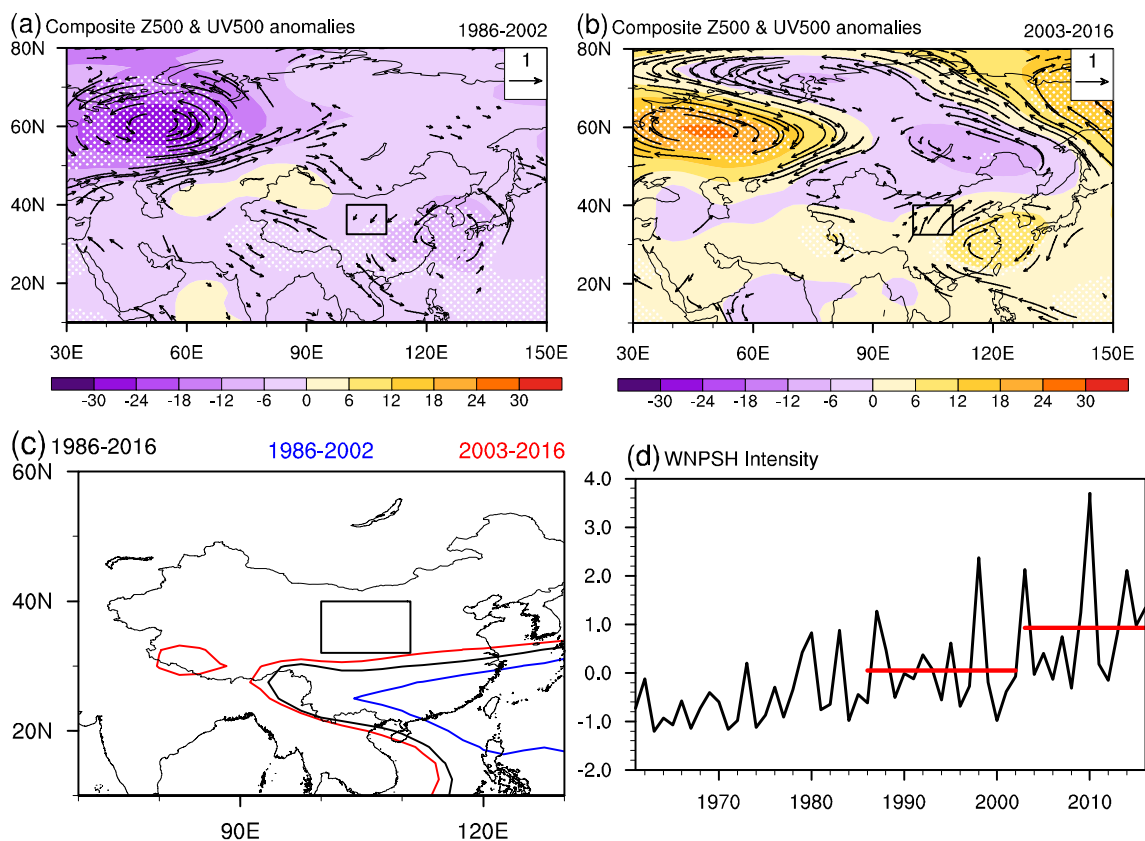|	Years
Decreased HP amount during 1986–2002	1986, 1987, 1989, 1991, 1993, 1994, 1996, 1997, 1999, 2000, 2002
Increased HP amount during 2003–2016	2003, 2008, 2009, 2010, 2011, 2012, 2013, 2014

Composite, correlation and regression analyses are employed to investigate the atmospheric circulation anomalies associated with HP events over NC China. Additionally, the Student's t test is used to detect the statistical significance in the correlation and regression analyses. Furthermore, the linear trends are eliminated before the correlation and regression analyses.

3 Results

### 3.1 Changes in Summer Heavy Precipitation Events at NC China

The summer precipitation at NC China shifts to increase around the mid-1970s, to decrease around the mid-1980s,

and to increase around the early 2000s (Fig. S1). Moreover, the average of HP intensity is 15.6 mm per day at NC China for 1961–2016, 15 times of that for summer mean precipitation. In general, the HP amount accounts for ~52% of the summer total precipitation (Fig. 1a), along with a correlation coefficient of 0.93 during 1961–2016. Specifically, the proportion has increased since the early 2000s. Figure 1b presents the time variation of the HP amount averaged within NC China during summer. It shows that the heavy precipitation amount exhibits significant inter-annual and inter-decadal changes in the last six decades. The result from the 7-year moving mean displays obvious shifts to increased heavy precipitation around the mid-1970s and the early 2000s, which is highly consistent with the variation of HP frequency (Fig. 1c). Similar results can be obtained from the

Fig. 3 Composite analysis of 500 hPa geopotential height (shaded; m) and horizontal wind (vectors; m s^{-1}) anomalies relative to the climatology: (**a**) less HP amount years during 1986–2002 and (**b**) more HP amount years during 2003–2016. (**c**) 5860-gpm mean position at 500 hPa in summer during 1986–2016 (black), 1986–2002 (blue), and 2003–2016 (red). Vectors that are less than 0.1 m s^{-1} are omitted.

Stippling areas (**a**, **b**) indicate values that significantly exceed the 90% confidence level, estimated using Student's t test. The rectangle represents the NC China. The climatology is the 1961–2016 average. (**d**) The time series of the Northwest Pacific Subtropical High intensity index from 1961 to 2016. The red horizontal lines represent the averages for 1986–2002 and 2003–2016, respectively
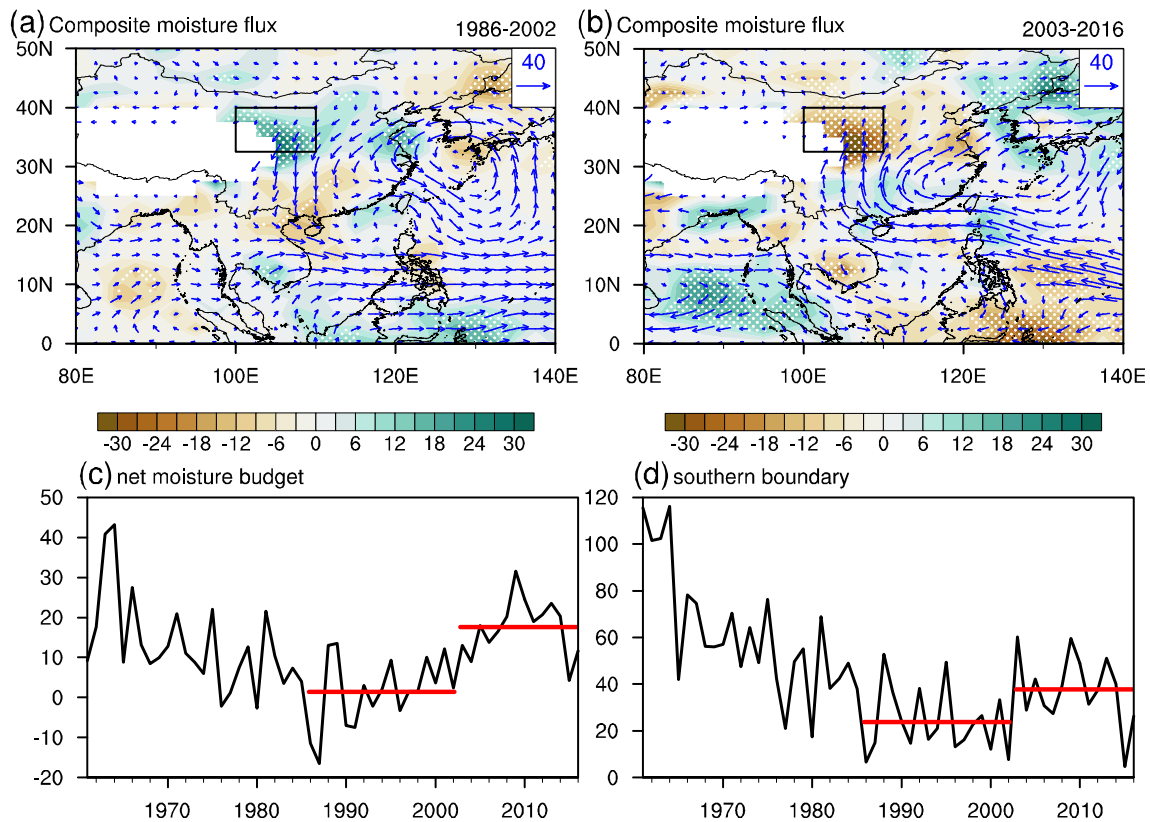
Fig. 4 Composite analysis of vertically integrated moisture flux (vectors; kg m^{-1} s^{-1}) and divergence (shaded; 10^{-6} kg m^{-2} s^{-1}) anomalies relative to the climatology: (**a**) less HP amount years during 1986–2002 and (**b**) more HP amount years during 2003–2016. The rectangle represents the NC China. Dotted areas indic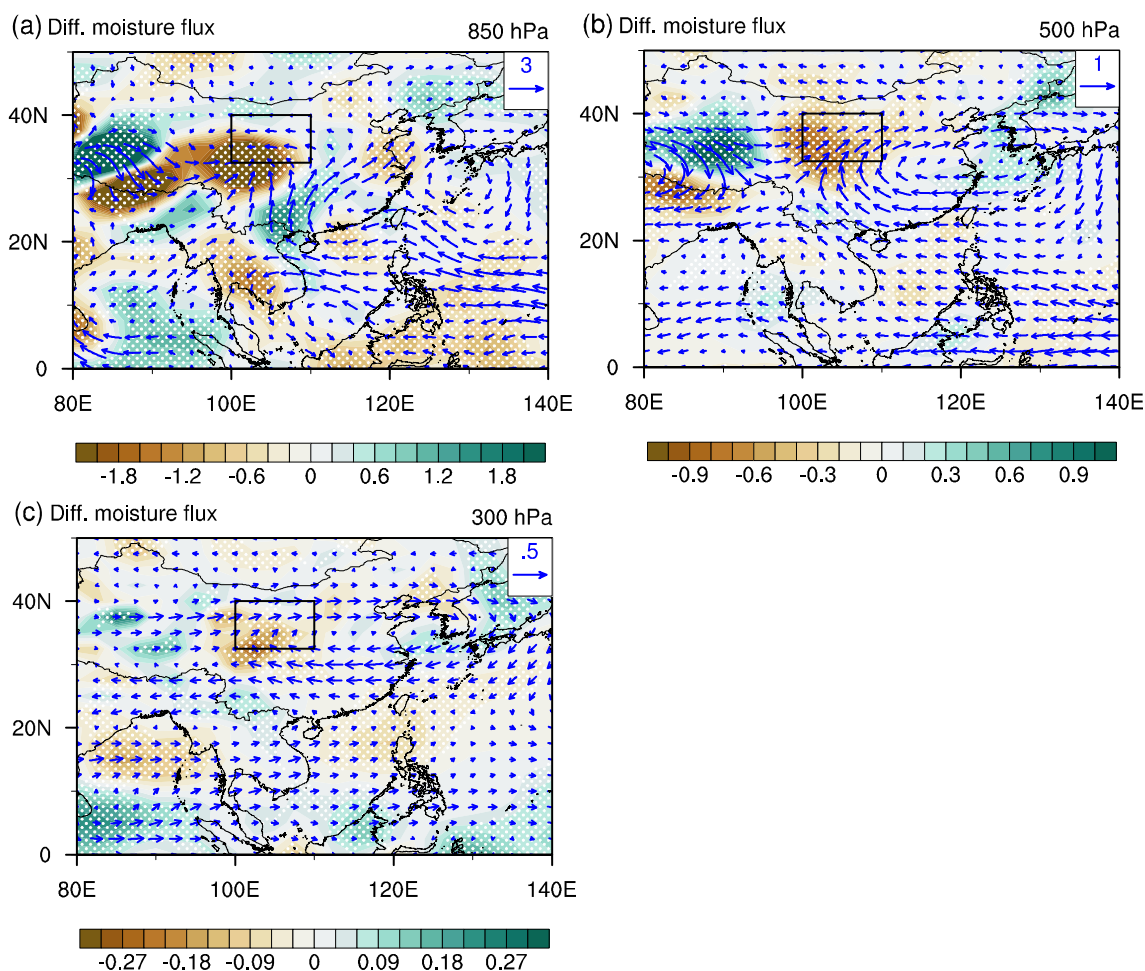ate values that significantly exceed the 90% confidence level, estimated using Student's *t* test. The climatology is the 1961–2016 average. (**c**) Time series of the net moisture budget averaged over NC China (10^6 kg/s). (**d**) Time series of the net moisture budget across the southern boundary (10^6 kg/s). The red horizontal lines represent the averages for 1986–2002 and 2003–2016, respectively

5- and 9-year moving means. Moreover, the detection of abrupt changes in the HP amount with a moving *t*-test indicates three significant inter-decadal changes around 1974, 1985 and 2002 (Fig. 1d), which can also be detected in the moving *t*-test on HP frequency (Fig. S2). Therefore, the changes in the HP amount are mainly attributed to the changes in HP frequencies, with a correlation coefficient of 0.91 during 1961–2016. Because of the fact that the recent decadal change of HP amount around the early 2000s is more significant than that around the mid-1970s, this study focuses on the most recent decadal change of HP amount over NC China. The following analysis is based on two periods: 1986–2002 (P1) and 2003–2016 (P2).The summer HP amount is increased by 24% from 127.0 mm per year during 1986–2002 to 156.9 mm per year during 2003–2016.

3.2 Changes in Atmospheric Circulation Associated with the HP Events

To explore the possible mechanism for the decadal change in HP events over NC China, the associated atmospheric circulation anomalies are first investigated. As shown in Fig. 2, the HP amount-related circulation anomalies display a barotropic structure. Increased HP amount features dominant positive height anomalies and anticyclonic wind fields over northern Europe, negative height anomalies and cyclonic wind fields centered over Lake Baikal, as well as positive values and anticyclone over the subtropical Northwest Pacific, displaying a Northwest-Southeast orientated wavelike pattern. The regimes could lead to remarkable low-level convergence and upper-level divergence anomalies and further trigger significant ascending motion over NC China (Fig. S3). The anomalous southerly at the western flank of the Northwest Pacific anticyclone and the westerly at the southern flank of the Lake Baikal cyclone transport water vapor across southern and western boundaries to NC China, respectively, contributing to profound moisture convergence anomalies in situ, which is consistent with previous studies (Sun and Wang 2014). Sun and Wang (2014) has found that the Eurasian continent, including southern and northwestern China as well as Central Asia, are main water vapor sources for NC China during summer half year. Consistently, HP events co-occur with profound moisture convergence anomalies over NC China and divergence anomalies over southern China and the adjacent waters (Fig. 2d). Sufficient moisture conditions and increased convection motion are favorable to heavy precipitation events.

Fig. 5 Differences in moisture transport (vectors; g s kg^{-1}) and divergence (shaded; 10^{-6} g s kg^{-1} m^{-1}) at (**a**) 850 hPa, (**b**) 500 hPa, and (**c**) 300 hPa between more HP amount years during 2003–2016 and less HP amount years during 1986–2002. The rectangle represents the NC China. Dotted areas indicate values that significantly exceed the 90% confidence level, estimated using Student's *t* test. The climatology is the 1961–2016 average

To illustrate the changes in HP amount-related atmospheric circulation anomalies, a composite analysis is performed for the years characterized by less HP amount during P1 and more HP amount during P2 (Table 1). More (less) HP amount years features above (below) than normal HP amount. Compared with the climatology, negative height anomalies dominate the Eurasian continent, co-occurring with anomalous cyclone centered over North Europe and anticyclone over Central Asia during P1 (Fig. 3a), which are unfavorable for heavy precipitation events. Northwesterly or northeasterly prevails over NC China, which is dry and cold. Additionally, the significant negative height and cyclonic wind field are centered at the Northwest Pacific, which suggests a weaker subtropical high than the climatology. It can be confirmed in Fig. 3c. It shows that the Northwest Pacific subtropical high (WNPSH) shifts eastward and southward during 1986–2002. However, after the early 2000s, the high over the North Europe strengthens and the low centering Lake Baikal deepens (Fig. 3b). In addition, positive height and anticyclonic wind anomalies appear

over the Northwest Pacific and East China. It implies that the WNPSH become intensified after the early 2000s, which is verified by the time variation of the WNPSH intensity index from the National Climate Center (Fig. 3d). Moreover, the WNPSH expands westward and northward during 2003–2016 (Fig. 3c). The southwesterly flow at the northwestern flank transport water vapor originating from southern China and the adjacent seas northward to NC China and facilitates more heavy precipitation.

Moisture plays a vital role in precipitation processes. The HP amount has an intimate linkage with the net moisture budget over the NC China, with a correlation coefficient of 0.57 during 1986–2016. Therefore, the changes in the moisture conditions are explored in this part. In comparison with climatology, the anomalous northerly flow means the weakened transport of water vapor to NC China during P1, along with anomalous moisture divergence and thus less HP amount (Fig. 4a). Nevertheless, the moisture divergence centered over the Northwest Pacific strengthens during P2. The anomalous
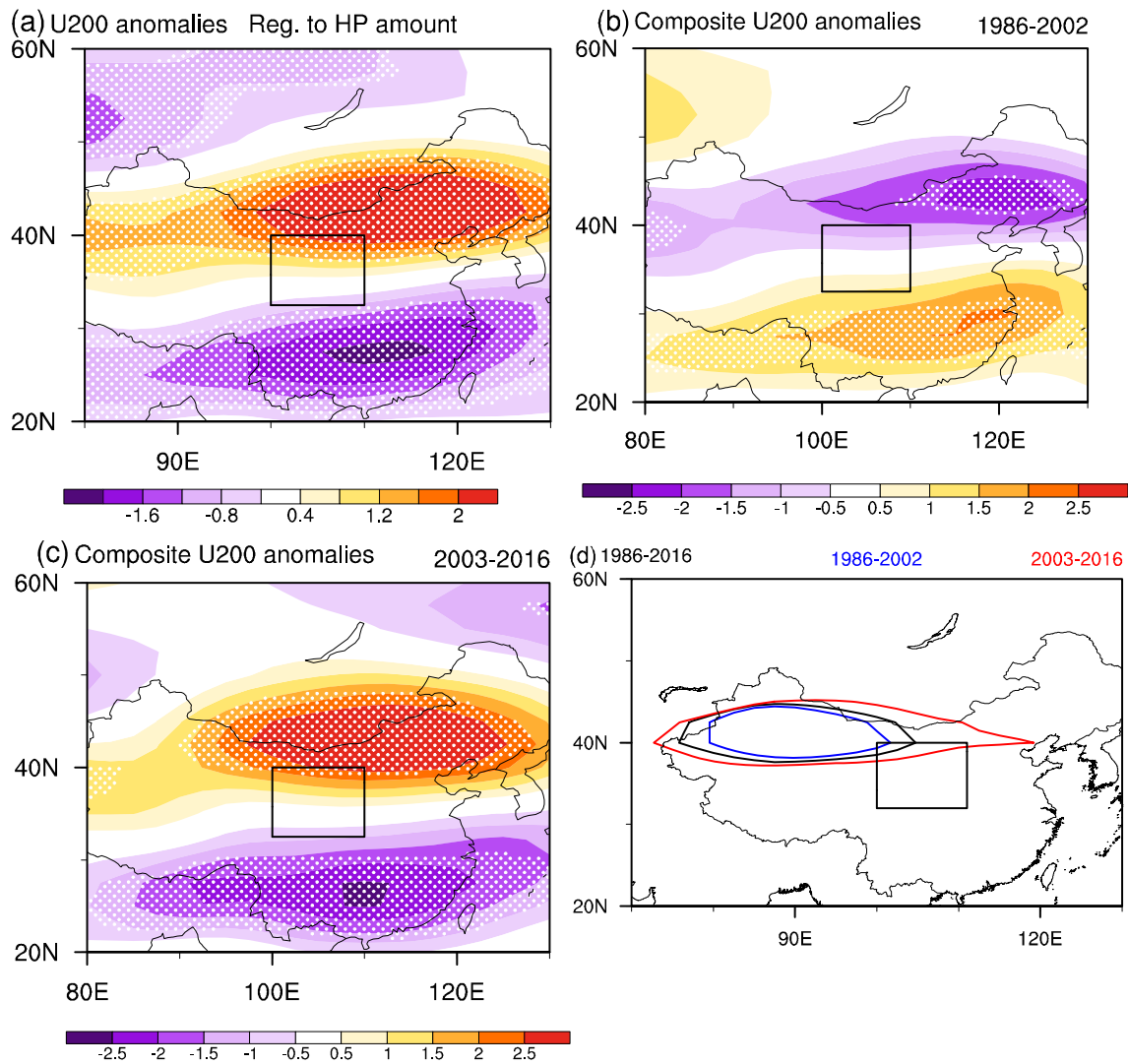
Fig. 6 (**a**) Linear regression of zonal wind at 200 hPa (m s^{-1}) with regard to HP amount during 1986–2016. Composite analysis of zonal wind at 200 hPa (m s^{-1}) relative to the climatology: (**b**) less HP amount years during 1986–2002 and (**c**) more HP amount years during 2003–2016. The rectangle represents the NC China. Dotted areas indicate values that significantly exceed the 90% confidence level, estimated using Student's *t* test. The climatology is the 1961–2016 average. (**d**) 30-m s^{-1} mean position of zonal wind at 200 hPa during summer for 1986–2016 (black), 1986–2002 (blue), and 2003–2016 (red)

southerly current at the western flank occupies southern China and transports water vapor deriving from South China Sea and southern China northward to NC China, inducing profoundly increased moisture convergence (Fig. 4b). Furthermore, anomalous moisture divergence prevails over Bay of Bengal, and the westerly current turns northward and transports water vapor from western Bay of Bengal to NC China. Accordant with the variation of the HP events, the net moisture budget has strengthened after the early 2000s (Fig. 4c). The net moisture flux increases from 1.45×10^6 kg/s during P1 to 17.6×10^6 kg/s during P2, suggesting that intensified moisture content contributes to increased frequency and amount of HP after the early 2000s. Moreover, the increment in the net moisture influx across the southern boundary accounts for 86% to that in the net moisture budget after the

early 2000s, along with an increase from 23.9×10^6 kg/s during P1 to 37.8×10^6 kg/s for P2 (Fig. 4d). The correlation coefficient of the net moisture influx across the southern boundary is 0.84 with the net moisture budget, and 0.57 with the HP amount during 1986–2016.

The differences of moisture transport at the lower, middle and upper troposphere between the two periods are further explored. Compared with the former period, significant anomalous divergence of moisture is centered at the western Bay of Bengal at 850 hPa after the early 2000s (Fig. 5a). The southwesterly flow at the northern flank, carrying warm moist current, turns southwesterly and invades NC China across southern boundary (Fig. 5a). Moreover, the southerly flow anomalies over eastern China transports water vapor deriving from southwestern China northward to NC China.
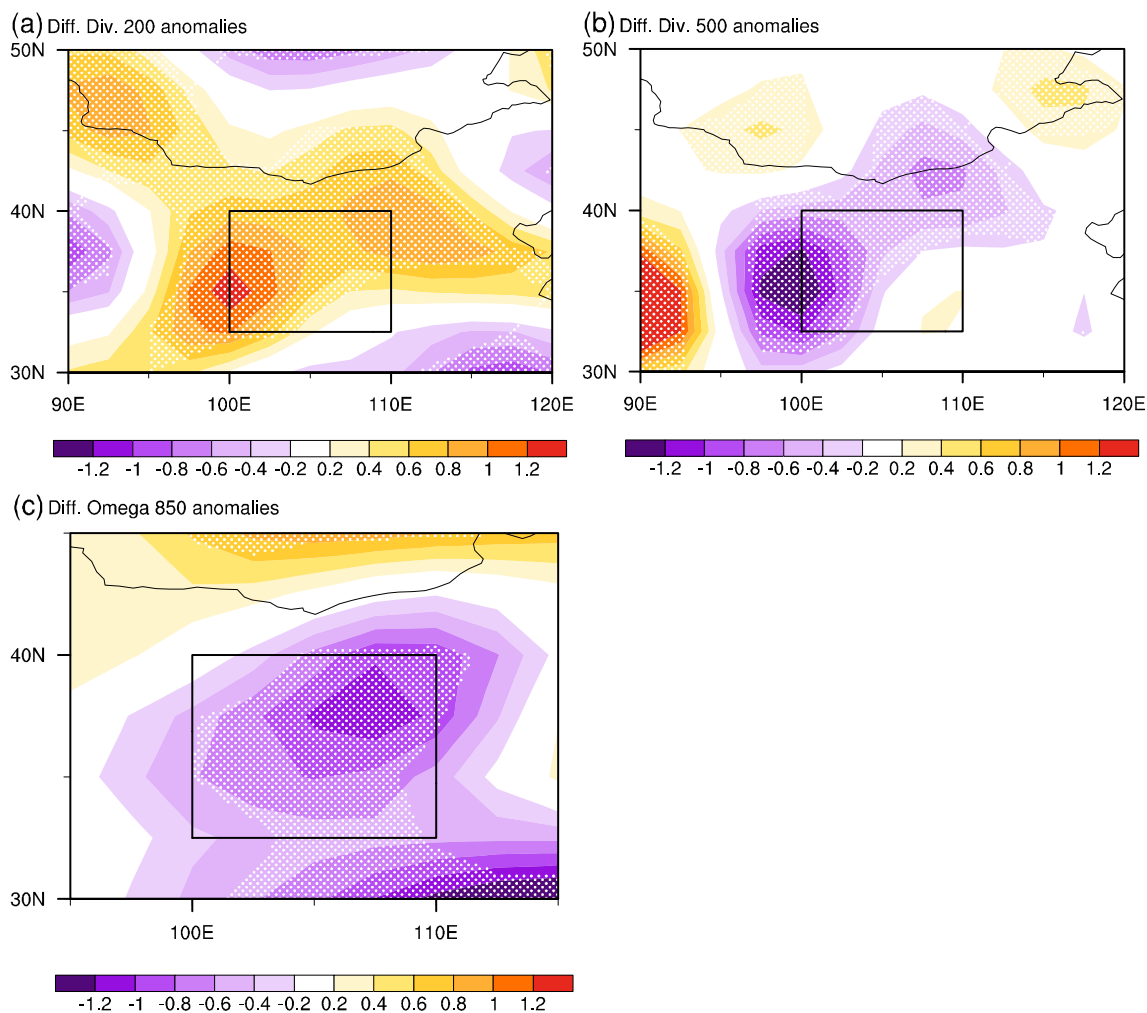
Fig. 7 Differences in horizontal divergence (10^{-6} s^{-1}) at (**a**) 200 hPa, and (**b**) 500 hPa, and (**c**) in vertical movement (10^{-2} Pa s^{-1}) between more HP amount years during 2003–2016 and less HP amount years during 1986– 2002. The rectangle represents the NC China. Dotted areas indicate values that significantly exceed the 90% confidence level, estimated using Student's *t* test

To a lesser extent, anomalous westerly flow crossing western boundary transport water vapor from West China eastward to NC China, which agrees with Sun and Wang (2014). These regimes contribute to a predominant convergence of moisture over NC China, facilitating more frequency and amount of heavy precipitation after the early 2000s than before. Furthermore, the moisture influx across the southern boundary at 850 hPa increases from 2.9×10^6 kg/s during P1 to 3.6×10^6 kg/s during P2. .

At the middle and upper levels, the net moisture flux across western boundary makes a greater contribution to the net moisture budget than the southern boundary. Specifically, the moisture influx across the western (southern) boundary increases from 1.2 (−0.3) $\times 10^6$ kg/s during P1 to 1.4 (0.1) $\times 10^6$ kg/s during P2 at 500 hPa, and the moisture influx across the western boundary increases by about 17% from 0.6×10^6 kg/s during P1 to 0.7×10^6 kg/s during P2 at 300 hPa. Correspondingly, stronger westerly or southwesterly currents prevail over NC China at middle and upper levels after the

early 2000s, inducing strengthened moisture convergence over NC China and divergence at western China after the early 2000s (Figs. 5b and c). These results suggest that the inter-decadal increase in net moisture budget over NC China is predominantly attributed to the increase in net moisture influx across the southern boundary at the lower level after the early 2000s. With a relatively smaller quantity, the increase of the net moisture influx across the western boundary at the middle and upper levels also contributes to the increase of the net moisture budget.

To understand the changes in the atmospheric circulation at the upper layer, the spatial distribution of the zonal wind at 200 hPa associated with HP events at NC China are shown in Fig. 6. Positive HP amount anomalies are concurrent with intensified westerly and easterly anomalies at north and south of 35°N, respectively (Fig. 6a). Compared with the climatology, the upper-level westerly (easterly) anomalies become weakened over North and Northeast China (southern China) during the early period (Fig. 6b). By contrast, the westerly and

easterly anomalies both become significantly stronger over northern and southern China after the early 2000s (Fig. 6c), respectively, favorable to HP events over NC China. Additionally, Du et al. (2008) revealed that East Asian westerly jet core facilitates horizontal divergence at its right side. Figure 6d depicts the positions of zonal wind at the value of 30 m / s. Compared with the climatology, the westerly jet stream region narrows westwards during P1, but expands eastwards during P2. Thus, the divergence circulation is more intense over NC China at the upper troposphere, inducing an intensified convergence at the lower layer and further exciting ascending movement in the latter period (Fig. 7).

4 Conclusions

This study investigates the recent interdecadal change in heavy precipitation events over northern Central China during summer and the associated atmospheric circulation anomalies. The HP amount shifts to increase during 2003–2016, compared with the period of 1986–2002, which is mainly attributed to the increased HP frequency. HP amount accounts for ~52% to total summer precipitation amount over NC China, and the most recent change in HP amount contributes to the inter-decadal increase in total summer precipitation at NC China after the early 2000s.

Compared with the early period, the Northwest Pacific subtropical high become intensified, and shifts westward and northward after the early 2000s. Consequently, significant moisture divergence anomalies appear Northwest Pacific, and convergence anomalies dominate NC China in the latter period. The net moisture budget dramatically increases after the early 2000s, which is generally attributed to the increased net moisture influx across the southern boundary. Further analysis shows that the strengthened southerly current, transporting water vapor derived from the western Bay of Bengal, southern China and adjacent seas northward to NC China across the southern boundary at the lower level, makes a dominant contribution to the moisture conditions. The enhanced westerly flow, transporting water vapor from West China eastward to NC China across the western boundary at the middle and upper layers, makes a lesser contribution to the increased net moisture budget. In addition, this inter-decadal change in HP events is also associated with the changes in the upper-level westerly jet. The westerly and easterly anomalies strengthen at the regions north and south to NC China after the early 2000s, respectively, along with the eastward expansion of westerly jet stream region during P2. Consequently, the lower-level convergence and upper-level divergence both intensify, and further trigger strengthened ascending movement. These conditions jointly contribute to strengthened HP events over NC China after the 2000s.

References

Chen, D.-D., Dai, Y.-J.: Characteristics of Northwest China rainfall intensity in recent 50 years (in Chinese). Chin J. Atmos. Sci. **33**, 923–935 (2009)

Du, Y., Zhang, Y.-C., Xie, Z.-Q.: Impacts of longitude location changes of east Asian westerly jet core on the precipitation distribution during Meiyu period in middle-lower reaches of Yangtze River valley. Acta Meteor. Sin. **66**, 566–576 (2008)

Kalnay, E., Kanamitsu, M., Kistler, R., et al.: The NCEP/NCAR 40-year reanalysis project. Bull. Amer. Meteor. Soc. **77**, 437–471 (1996)

Jiang, Z.-H., Yang, J.-H., Zhang, Q.: Influence study of spring Indian SSTA to summer extreme precipitation events the eastern part of Northwest China. J. Tropical Meteor. **25**, 642–648 (2009)

Liu, X.-Y., Wang, J.-S., Li, D.-L., et al.: Interannual and interdecadal atmospheric circulation anomalies of autumn dry/wet over the loess plateau and its multi-scalar correlation to SST (in Chinese). Acta Phys. Sin. **62**, 1–15 (2013)

Liu, Y., Du, C.-L.: Diagnostic study on an abrupt heavy rainstorm process in the loess plateau (in Chinese). Plateau Meteor. **25**, 302–308 (2006)

Ran, J.-J., Ji, M.-X., Huang, J.-P., et al.: Characteristics and factors of climate change in arid and semi-arid areas over northern China in the recent 60 years (in Chinese). J. Lanzhou University (Natural Sci.). **50**, 46–53 (2014)

Simmonds, I., Bi, D.-H., Hope, P.: Atmospheric water vapor flux and its association with rainfall over China in summer. J. Clim. **12**, 1353–1367 (1999)

Sun, B., Wang, H.-J.: Moisture sources of semiarid grassland in China using the Lagrangian particle model FLEXPART. J. Clim. **27**, 2457–2474 (2014)

Sun, B., Wang, H.-J.: Analysis of the major atmospheric moisture sources affecting three sub-regions of East China. Int. J. Climatol. **35**, 2243–2257 (2015a)

Sun, B., Wang, H.-J.: Inter-decadal transition of the leading mode of inter-annual variability of summer rainfall in East China and its associated atmospheric water vapor transport. Clim. Dyn. **44**, 2703–2722 (2015b)

Sun, B., Zhu, Y.-L., Wang, H.-J.: The recent Interdecadal and interannual variation of water vapor transport over eastern China. Adv. Atmos. Sci. **28**, 1039–1048 (2011)

Sun, W.-Y., Mu, X.-M., Song, X.-Y., et al.: Changes in extreme temperature and precipitation events in the loess plateau (China) during 1960–2013 under global warming. Atmos. Res. **168**, 33–48 (2016)

Tan, L.-C., An, Z.-S., Huh C.A., et al.: Cyclic precipitation variation on the western Loess Plateau of China during the past four centuries. Scientific Reports. **4**, 6381 (2014)

Wan, L., Zhang, X.-P., Ma, Q., et al.: Spatiotemporal characteristics of precipitation and extreme events on the loess plateau of China between 1957 and 2009. Hydr. Processes. **28**, 4971–4983 (2014)

Wang, H.-J., Fan, K.: Central-North China precipitation as reconstructed from the Qing dynasty: signal of the Antarctic atmospheric oscillation. Geophys. Res. Lett. **32**, L24705 (2005)

Wang, H.-J., Zhang, Y.: Model projections of east Asian summer climate under the 'free Arctic' scenario. Atmos. Oceanic Sci. Lett. **3**, 176–180 (2010)

Wang, P.-X., He, J.-H., Zheng, Y.-F., et al.: Inter-decadal relationships between summer Arctic oscillation and aridity-wetness feature in Northwest China(in Chinese). J. Desert Res. **27**, 883–889 (2007)

Wei, N., Gong, Y.-F., Sun, X., et al.: Variation of precipitation and water vapor transport over the Northwest China from 1959 to 2005(in Chinese). J. Desert Res. **30**, 1450–1457 (2010)

Wu, F.-T., Fu, C.-B.: Change of precipitation intensity spectra at different spatial scales under warming conditions. Chin. Sci. Bull. **58**, 1385–1394 (2013)

Wu, J., Gao, X.-J.: A gridded daily observation dataset over China region and comparison with the other datasets. Chinese. J. Geophys. **56**, 1102–1111 (2013)

Xu, H.-L., Feng, J., Sun, C.: Impact of preceding summer North Atlantic oscillation on early autumn precipitation over Central China. Atmos. Oceanic Sci. Lett. **6**, 417–422 (2013)

Xu, J.-Y., Shi, Y., Gao, X.-J.: Changes in extreme events as simulated by a high-resolution regional climate model for the next 20–30 years over China. Atmos. Oceanic Sci. Lett. **5**, 483–488 (2012)

Yuan, H.-Y., Hou, J.-Z., Du, J.-W., et al.: The climate characteristics of Sudden local storms in Loess Plateau. J. Catastrophology. **22**, 101–104, 113 (2007)

Publisher's Note Springer Nature remains neutral with regard to jurisdictional claims in published maps and institutional affiliations.